

# Inferring Properties of the ISM from Supernova Remnant Size Distributions

Benjamin D. Elwood,<sup>1</sup>★ Jeremiah W. Murphy,<sup>1</sup>† Mariangelly Díaz-Rodríguez<sup>1</sup>

<sup>1</sup>*Department of Physics, Florida State University, Tallahassee, FL 32306*

Accepted XXX. Received YYY; in original form ZZZ

## ABSTRACT

We model the size distribution of supernova remnants to infer the surrounding ISM density. Using simple, yet standard SNR evolution models, we find that the distribution of ambient densities is remarkably narrow; either the standard assumptions about SNR evolution are wrong, or observable SNRs are biased to a narrow range of ambient densities. We show that the size distributions are consistent with log-normal, which severely limits the number of model parameters in any SNR population synthesis model. Simple Monte Carlo simulations demonstrate that the size distribution is indistinguishable from log-normal when the SNR sample size is less than 600. This implies that these SNR distributions provide only information on the mean and variance, yielding additional information only when the sample size grows larger than  $\sim 600$  SNRs. To infer the parameters of the ambient density, we use Bayesian statistical inference under the assumption that SNR evolution is dominated by the Sedov phase. In particular, we use the SNR sizes and explosion energies to estimate the mean and variance of the ambient medium surrounding SNR progenitors. We find that the mean ISM particle density around our sample of SNRs is  $\mu_{\log n} = -1.33$ , in  $\log_{10}$  of particles per cubic centimeter, with variance  $\sigma_{\log n}^2 = 0.49$ . If interpreted at face value, this implies that most SNRs result from supernovae propagating in the warm, ionized medium. However, it is also likely that either SNR evolution is not dominated by the simple Sedov evolution or SNR samples are biased to the warm, ionized medium (WIM).

**Key words:** (ISM:) supernova remnants – methods:analytical – methods:numerical – methods:statistical

## 1 INTRODUCTION

### 1.1 Motivation

The evolution and properties of Supernova Remnants (SNRs) are useful in studying the physics of the interstellar medium, as well as their respective progenitor stars. While the evolution of their expansion has been studied for half a century, more recent efforts have focused on the statistics of their size distributions and progenitor masses (Gogarten et al. 2009; Badenes et al. 2010; Murphy et al. 2011; Asvarov 2014; Jennings et al. 2012, 2014; Williams et al. 2014). For example, one may characterize the age of SNRs, thereby inferring the age of the star that exploded and its progenitor mass. Because SNRs last far longer than SNe themselves, there are far more observable SNRs in a galaxy than SNe. Therefore, SNR catalogs are important tracers of recent SNe, for both Ia and CCSN. Badenes et al. (2010), for example, used SNRs to constrain the delay time distribution for SN Ia. Jennings et al. (2012) and Jennings et

al. (2014) combined SNR data from M31 and M33 to obtain a distribution of progenitor masses for core-collapse supernovae. Using 115 SNRs, they found a clear minimum mass for CCSNe of  $7.3 M_{\odot}$ . Interestingly, they also found far fewer high mass progenitors compared to the Salpeter IMF. This suggests that either the most massive stars do not explode as supernovae or that selection effects bias against finding SNRs in the youngest regions. Given this result, we are motivated to understand the environments surrounding these SNRs and infer any potential biases in the SNR catalogs.

In this paper, we investigate whether there is a bias for finding SNRs in certain environments. Our approach will be to use statistical analyses of the SNR size distributions  $N(< D)-D$  for M31 and M33 ( $N$  being number and  $D$  diameter). In principle, the size of a supernova remnant depends upon explosion energy, age, and the density of the interstellar medium. Thus, the distribution of SNR sizes depends upon the distribution of ISM densities; any bias affecting SNR catalogs might therefore manifest itself in the distribution of densities.

Two approaches can be employed to determine whether a significant bias exists. One is to model the observations including bias,

★ bde14b@my.fsu.edu, jwmurphy@fsu.edu

and the other is to model the observations excluding the bias and test its consistency with other observations. If the model without bias is shown to be inconsistent with other observations, then one can be confident that there must be a significant bias. Modeling the bias is often the preferred option; however, this can be complex and adds many unconstrained parameters to the modeled data (Sarbadhicary et al. 2017). Presently, modeling SNR evolution and visibility requires many uncertain model parameters for which there are only a handful of observables (such as diameter and radio luminosity). Therefore, the first step is to show that there is a bias, with the simplest and least complex method being to attempt to model the SNR evolution and infer the ISM density without the bias. If the resulting inference does not match expectations of ISM density from other observations and simulations, then this effectively rules out the model without a bias and suggests a strong bias.

Sarbadhicary et al. (2017) present the most recent and comprehensive attempt regarding these efforts by modeling the radio emission and observable lifetimes of SNRs, a necessary step in understanding the bias in SNR catalogs. However, modeling the SNR radio emission relies heavily on correctly modeling cosmic ray particle production, SNR evolution, cosmic ray feedback, and synchrotron emission. Due to the many uncalibrated parameters in each of these steps, there is a danger that the inferred conditions will be heavily influenced by the assumed priors for each of these parameters; with so many parameters, it will be difficult to falsify the predictions. Nonetheless, as Sarbadhicary et al. (2017) demonstrate, modeling the radio emission and observable lifetimes will be important for properly constraining the SNR evolution. Therefore, it will be important to constrain the many parameters in the radio emission models.

While the important work of calibrating the radio emission continues, there is another approach to assessing the bias that is simpler and leads to clear, falsifiable predictions. In this work, we simply model the SNR evolution with the standard assumption that all SNRs are observed in the Sedov phase of expansion with an observable lifetime that is determined by the onset of the radiative phase. The simplicity of the model, due to very few parameters, offers clear and directly falsifiable results. Even in the event that the inferred densities are falsified, we are certain to learn that obvious and standard assumptions about SNR evolution are seriously mistaken. Such a result would greatly illuminate the role of bias in SNR catalogs.

## 1.2 Background

For decades, there have been several attempts to infer the properties of the ISM based upon SNR size distributions (Fusco-Femiano & Preite-Martinez 1984; Berkhuijsen 1986, 1987; Badenes et al. 2010; Asvarov 2014). This was motivated, in part, by an early analysis of size distributions in the Magellanic Clouds by Mathewson et al. (1983) in which the authors observed a linear  $N$ - $D$  cumulative distribution, more consistent with the free expansion phase than Sedov phase. Assuming a single explosion energy and ISM density, this is at odds with a distribution ( $N \sim D^{2.5}$ ) expected for the Sedov phase (Mathewson et al. 1983). Instead, a linear cumulative distribution is most consistent with the free expansion phase of evolution. Considering that free expansion takes place within a short time frame ( $t_{FE} \sim 10^2$  yr), this interpretation seems unlikely. For example, the short timescale for the free expansion phase would suggest far fewer SNRs per galaxy than are actually observed. The SN rate for a typical  $L^*$  galaxy is 1/100 years (Cappellaro et al. 1999; Faucher-Giguère & Kaspi 2006; Li et al. 2011), implying that

if free expansion phase dominates, one should only observe  $\sim 1 - 10$  SNRs per galaxy at any given time. Yet, SNR catalogs for nearby galaxies contain about 100 SNRs, which is more consistent if one considers the longer Sedov phase.

Shortly after the findings presented by Mathewson et al. (1983), Hughes et al. (1984) argued that those proposing a free expansion interpretation did not carefully consider how selection effects, explosion energies, or ISM densities could influence the diameter distributions and instead showed that a linear relationship was more consistent with Sedov evolution. No doubt influenced by this work, more contemporary analyses were provided for both M33 and M82 by Bandiera & Petruk (2010) and for the Small and Large Magellanic Clouds by Badenes et al. (2010). Bandiera & Petruk (2010) state that a linear cumulative distribution does not imply free expansion, if caused by a combination of SNR data expanding into different ambient densities. Similarly, since SNRs in free expansion can experience shock velocities up to  $\sim 10^4$  km/s, those expanding to a diameter of up to 60 pc (a maximum first obtained by Mathewson et al. (1983)) would have thousand-year timescales. This result leads to both a highly-overestimated SN rate (as discussed earlier) and low-limit progenitor mass when compared to SNR data from any known galaxy (Maoz & Badenes 2010). In light of these contradictions, contemporary views hold that most observed SNRs are in the Sedov phase of expansion (Lee & Lee 2014).

Fusco-Femiano & Preite-Martinez (1984) showed that the SNR data could be replicated with Sedov theory by rejecting a large-scale homogeneous ISM and incorporating a spread of densities in their calculations. Additionally, the completeness of SNR data became an increasingly important factor in whether or not erroneous assumptions were made regarding free expansion. Berkhuijsen (1986, 1987) continued this investigation by recognizing a difficulty in “proving” SNRs to be in free expansion: SNR diameter distributions are statistically vulnerable to outside influences from ambient density or explosion energy. Thus, a supporting expansion law can be obscured by any variation in parameters that randomize the SNR diameters. Additionally, via Kolmogorov-Smirnov analyses, the author concluded that neither a free expansion nor Sedov expansion power law could be satisfactorily rejected, based upon a lack of completeness in the SNR data (Berkhuijsen 1987). As SNR data has become more readily available, due to surveys such as Lee & Lee (2014) for M31 and Long et al. (2010) for M33, this problem has been somewhat ameliorated and support for a free expansion observation has declined. As we will demonstrate shortly, diameter distributions appear to be closer to log-normal in nature, rendering a linear distribution only approximately valid within a certain range.

A more recent motivation for studying SNR distributions was provided by Badenes et al. (2010), whose analysis included a discussion of the SNR size distributions for the SMC and LMC. Having gathered 77 multi-wavelength SNRs, the authors argued for an approximately-linear characterization up to a diameter of 60 pc, stating that this behavior is determined by the physics of the SNR interaction with the interstellar medium. Their model suggests that SNRs expanding beyond this diameter exit the Sedov phase of expansion to the radiative, quickly fading from detection with a lifetime that depends upon the surrounding ISM density. The authors note that a linear size distribution can arise naturally if the distribution of ISM densities follows a power law with an exponent of  $-1$  with a wide range of densities.

Analyses of this nature suggest an important hypothesis: size distributions of supernova remnants appear to hold clues as to the ISM environments in which they propagate. Motivated by this possibility, we have initiated a statistical analysis of our own, thanks to

external data provided by Lee & Lee (2014) for M31 and Long et al. (2010) for M33. As we show in section 2, we note that these size distributions are log-normal, which is a natural consequence of Sedov expansion. From this, we derive a distribution of ISM densities, allowing us to extract useful statistics on the SNR environments by applying the Central Limit Theorem.

In order to understand the size distribution of SNRs, it is essential to understand the dynamics of SNR evolution, particularly lifetimes. It is often assumed (but not explicitly verified) that the dominant, observable phase of an SNR is given by the Sedov-Taylor solution. This is because the observable timescales of both the free expansion ( $t_{FE} \sim 10^2$  yr) and radiative phase are too short to be adequately detected. Considering that the cooling time for a given ISM density goes as  $t_{cool} \sim \rho^{-1}$  (Truelove & McKee 1998; Blondin et al. 1998), SNRs in the radiative phase can quickly fade from view, especially if merging with dense environments. Entry into the radiative phase allows for brief X-ray detection, after which the threshold becomes too low for reliable observation, despite the fact that radiative lifetimes can similarly last for thousands of years (Cioffi et al. 1988; Blondin et al. 1998). Therefore, we assume the maximum time to observe an SNR to be approximately equal to the maximum Sedov lifetime, at which the cooling lifetime becomes equal to the expansion time for a SNR:

$$t_{max} \sim R_{max}^{5/2} \rho^{1/2} E^{-1/2} \quad (1)$$

We derive this in the equation for its namesake radius, up to a dimensionless constant:

$$R \sim E^{1/5} t^{2/5} \rho^{-1/5} \quad (2)$$

where  $E$  is the explosion energy of the progenitor star, often being on the order of  $10^{51}$  ergs.

Assuming the Sedov phase to be the simplest and most natural phase affords us a useful avenue to proceed. We analyze the statistics of SNR size distributions to infer properties of the SNR Sedov variables, such as the ambient density. As will be shown in the next section, the size distributions for radii closely match a log-normal distribution for our sample sizes ( $N \sim 10^2$ ). Interest in this observation stems, in part, from the Central Limit Theorem (CLT) which states, roughly, that the average of a sum of a large number of random, independently-distributed variables will be approximately normal, regardless of the underlying distribution. By extension, when the logarithm of a product of such variables approaches a normal distribution, the product itself is a log-normal distribution. For the Sedov radius, eq. 2:

$$\log R \sim \frac{1}{5} (\log E + 2 \log t - \log \rho) \quad (3)$$

log-normality exists conditionally if the energy, ISM density, and SNR lifetime are independently distributed and have well-defined means and variance. In fact, it is this condition that bears the most relevance to this paper; conversely speaking, if a log-normal distribution is obtained from some sample, one is able to extract statistically meaningful information on the mean and variance of the random variables. For the purpose of our study, we seek to extract such information on the ISM density to see if SNR surveys are biased towards particular environments.

Considering that the Central Limit Theorem holds only for many random, independent variables, it is clear that our analysis will be valid only within a certain criteria. The Sedov radius contains only three variables (energy, density, lifetime), with the lifetime being *dependent* upon explosion energy and density. This likely plays a role in our simulated distributions being inconsistent with

log-normal above a certain sample size, roughly 600 SNRs (to be shown later). However, statistics suggest that our simulations are consistent with the M31 and M33 data below this threshold, thereby making our analysis approximately valid within the CLT context.

This paper begins by presenting size distributions of previous M31 (Lee & Lee 2014) and M33 data (Long et al. 2010), for a total of 187 SNRs. We suggest in Section 2 that a log-normal relationship for the diameter (or radius) is most appropriate, in contrast to previous attempts characterizing it as linear, such that we are naturally led to considering the statistical consequences of the Central Limit Theorem for the Sedov variables. We then proceed, in Section 3, to Monte Carlo simulations of the Sedov radius by modeling the blast energy, SNR lifetime, and ambient density as random variables. We see that, for  $N \sim 10^2$ , a log-normal distribution is similarly obtained, to be lost only when  $N$  grows large. To acquire more detailed information, we then employ a Bayesian inference scheme (Foreman-Mackey et al. 2013), assuming a Gaussian log-likelihood, for the purpose of obtaining means and variance for the Sedov variables. Our central result is that our analyses point to an intriguingly low variance for the ISM density ( $\sigma^2 = 0.49$ ); this suggests that SNR surveys are presently biased towards rather uniform environments, most likely the warm, ionized medium. These results are consistent with other recent efforts suggesting narrow density distributions (Gatto et al. 2016; Sarbadhicary et al. 2017). The reason for such is unknown, though we offer possible explanations in our discussion, one being that the lower-end of size distributions suffers a cutoff resulting from stellar cavities formed from pre-explosion solar wind of the progenitor star. We propose alternative corrections to our Sedov model to account for SNR interactions with the stellar wind and surrounding ISM. Our findings are then summarized in the conclusion.

## 2 DATA AND STATISTICS

### 2.1 SNR Data

One of our primary motivations in considering the size distribution of SNRs is to assess whether there are biases in the SNR catalogs used by Jennings et al. (2012, 2014). Therefore, in this analysis we focus on those catalogs, which includes SNR data from M31 and M33. The M31 data includes a fairly new, optically selected survey by Lee & Lee (2014), inspired by previous efforts from Braun & Walterbos (1993); Magnier et al. (1995); Williams et al. (2014) and using data from the Local Group Survey (Massey et al. 2006). For both M31 and M33, SNR identification was done using [SII]:H $\alpha$  ratios (Gordon et al. 1998); objects identified with ratios exceeding 0.4 fall into the category of SNRs. Then, to verify the SNRs, these authors used radio and X-ray data to confirm their SNR status (Lee & Lee 2014; Long et al. 2010).

Long et al. (2010) considered it likely that observational and physical selection effects contribute to the shape of SNR distributions. From an observational standpoint, the authors mention a tendency to focus on isolated objects, whose shells are easily distinguishable, as well as a bias towards objects whose optical diameters were below 10" (a result of data sensitivity to beam diameter). As detection probabilities for large-diameter SNRs are lower than small-diameter ones, this is always an effect to consider when evaluating SNR data sets. However, Jennings et al. (2014) suggests that selection effects related to detection methods do not significantly contribute to SNR catalogs, though they admit to leaving this as a somewhat open-ended question. In addition to observational biases,

Long et al. (2010) also discusses the aforementioned physical effect in which SNRs that explode into dense ISM environments will dissipate much more rapidly, escaping detection (see eq. 12). Jennings et al. (2014) likewise mentions the possibility that any SNR cataloger biased towards particular progenitors or ISM environments could affect the overall distribution shape. Thus, understanding the nature of the bias involved in the relationship between SNRs and the ISM is not only of theoretical interest, but is a realistic problem in SNR observation.

It is important to mention that this work provides no distinction between CCSN and Type Ia SNR candidates. Recent works suggest that while CCSNe dominate SNR samples, the fraction of Type Ia SNe are not negligible and typically constitute roughly a quarter of total SNe (Li et al. 2011; Lee & Lee 2014; Sarbadhicary et al. 2017). Jennings et al. (2014) in particular provide support for 25% being an upper limit on Type Ia identification, both due to differences in surface brightness, as compared to CCSNe, and spatial distributions. Eventually, one should make a distinction between SNRs from CCSNe and SN Ia, as there could be a difference in the ISM properties associated with each. Sarbadhicary et al. (2017) attempted to model the SNR size distribution including both SNIa and CCSNe, but this requires yet another uncertain parameter, the fraction of SNIa compared to total. This fraction is very difficult to determine from the properties of SNRs in external galaxies. The best method is to age-date the surrounding stellar population for each SNR, an analysis that will come in due time. Until then, we are forced to treat the entire SNR population as a whole. Therefore, we will be inferring the surrounding ISM density distribution for both CCSNe and SNIa.

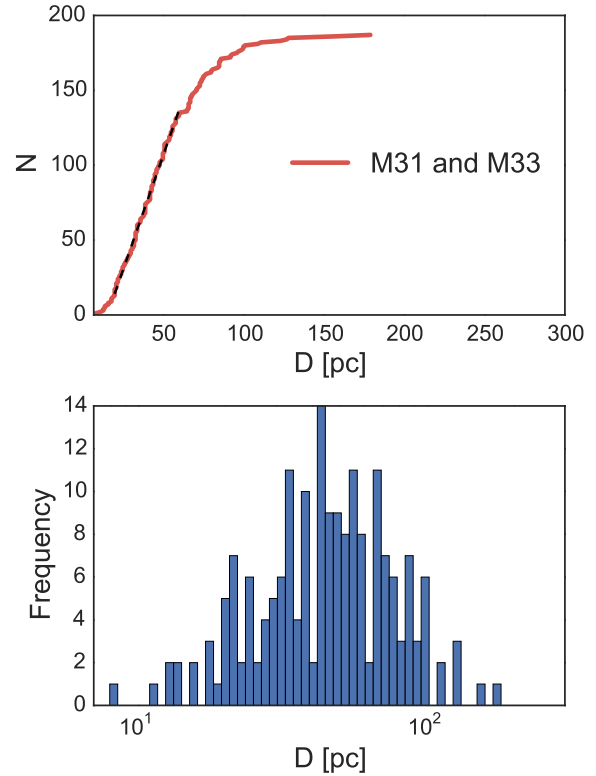
## 2.2 Size Distributions

Figure 1 presents the size distributions for M31 and M33 SNRs; the top panel shows the cumulative distribution and the bottom panel shows the frequency distribution. By plotting the frequency distribution in the log, it is easy to see that the size distribution is consistent with a log normal distribution. To allay statistical concerns with mixing our M31 and M33 samples, we performed a simple Kolmogorov-Smirnov test between the two sets to obtain a P-value of  $\approx 0.146$  to verify that both samples could come from the same underlying distribution, thereby justifying a combined data set.

In the past, others assumed that linear distributions implied a detection of SNRs in their free expansion phase, though, as mentioned previously, this view is no longer shared. A simple reason for this is that the timescale for free expansion can only last for a hundred or so years. The transition from free expansion to the Sedov phase begins when the swept-up mass roughly equals the ejecta mass,  $M_{ej} \sim M_s \sim R^3 \rho$ ; with a blast energy of  $10^{51}$  erg, progenitor mass of  $8M_{\odot}$ , and an ISM particle density of  $0.1 \text{ cm}^{-3}$ :

$$t \sim E^{-1/2} M^{5/6} \rho^{-1/3} \sim 10^2 [\text{yr}] \quad (4)$$

Assuming free expansion also contradicts the observed SNR data for the Magellanic Clouds, now believed to be in the adiabatic (Sedov) phase of expansion (Badenes et al. 2010). In this work, we not only assume SNRs to be in the Sedov phase of expansion, but propose that a Gaussian distribution fully encapsulates the observed data, motivated largely by the obviously log-normal shape of the histogram in Figure 2.



**Figure 1.** (above) Cumulative distribution for both M31 and M33 SNR data. Dashed line indicates linear characterization for SNRs up to the “cutoff diameter” of 60 pc. Ignoring the rest of the data leads to assuming a linear distribution and the erroneous interpretation of free expansion. (below) Histogram for M31 and M33 in log space; log-normality is present with P-value  $\approx 0.277$ , a consequence of Sedov phase expansion.

## 2.3 Density Distribution Statistics

We can easily model the distributions of dependent variables by approximating the SNR distributions as log-normal. By doing so, we extract meaningful statistics of these variables, such as inferring properties of the ISM. First, recall the Central Limit Theorem, which states that, for a sufficiently large number of random, independent variables (with well-defined means and variance), the mean of a large number of iterates will be normally distributed. By extension, when the logarithm of a product of such variables (taking positive values only) approaches a normal distribution, the product itself is log-normally distributed.

We extend these statistical properties to the Sedov radius (eq. 2), a product of energy, time, and interstellar density. Since the SNR diameters are log-normally distributed, we can extract statistical information on the mean and variance, specifically the ISM density. We first note that the variance of our given data for  $\log R$  is quite small; it then becomes easy to calculate a quick estimate of the maximum variance for  $\log \rho$  if we assume the Sedov variables to be independently-distributed. For the Sedov radius, our mean and variance (in the log) are:

$$\overline{\log R} = \frac{1}{5} \left( \overline{\log E} + 2\overline{\log t} - \overline{\log \rho} \right) \quad (5)$$

$$\sigma_{\log R}^2 = \left( \frac{1}{5} \right)^2 \sigma_{\log E}^2 + \left( \frac{2}{5} \right)^2 \sigma_{\log t}^2 + \left( \frac{1}{5} \right)^2 \sigma_{\log \rho}^2 \quad (6)$$

To calculate an upper bound on the density in the variance, we set the other two variables to zero. Then, we obtain the largest possible variance for the log-density:

$$\sigma_{\log \rho}^2 = 25\sigma_{\log R}^2 \quad (7)$$

Observationally, the variance for the radius is  $\sigma_{\log R}^2 \approx 0.055$ , thus setting an *upper limit* for the density variance  $\sigma_{\log \rho}^2 = 1.375$ . This exercise is indeed simplified, for cross-terms such as the lifetime depend upon, for example, the blast energy and ISM density. Nonetheless, the exceptionally small variance suggests that a more thorough analysis, which we present in the next section, will produce an exceptionally narrow distribution for densities.

### 3 SIMULATIONS

We seek to infer the distribution of densities surrounding the SNRs by invoking a model that translates the distribution of densities into a distribution of SNR sizes. We use Monte Carlo simulations modeling the explosion energy  $E$ , progenitor mass  $M$ , and ambient ISM density  $\rho$  as random variables in the form of power laws:

$$\rho = \rho_+^R \rho_-^{1-R} \quad (8)$$

$$E = E_+^Q E_-^{1-Q} \quad (9)$$

$$t = S(t_+ - t_-) + t_- \quad (10)$$

$$\left( W(M_+^{-1.35} - M_-^{-1.35}) + M_-^{-1.35} \right)^{-1/1.35} \quad (11)$$

where  $Q$ ,  $R$ ,  $S$ , and  $W$  are random numbers that range from 0 to 1 and the  $+$  and  $-$  indicate maximum and minimum values, respectively (with progenitor mass ranging from one to one hundred solar masses). We now consider the SNR cooling time for a given ISM density:

$$t_{cool} \sim \frac{kT}{\rho \Lambda(T)} \quad (12)$$

with  $\Lambda(T)$  being the cooling function as provided by [Truelove & McKee \(1998\)](#) and [Blondin et al. \(1998\)](#). Assuming a Sedov model in conjunction with eq. 12 leads to the maximum radius as found in [Bandiera & Petruk \(2010\)](#):

$$R_{max} \sim E^{(3-2\epsilon)/(11-6\epsilon)} \rho^{-(5-2\epsilon)/(11-6\epsilon)} \quad (13)$$

after which the SNR enters the radiative phase and fades from view. The exponent  $\epsilon$  arises from assuming a cooling function of the form  $\Lambda(T) \sim T^\epsilon$  as found in [Truelove & McKee \(1998\)](#) where, for our simulations,  $\epsilon = 0.5$ .

The result of these Monte Carlo simulations is displayed in Figure 2, where we are able to reproduce the log-normal behavior for  $N = 300$ , with  $N$  being the number of simulated SNRs. However Figure 2 shows that the size distributions are clearly non-Gaussian for large  $N$ . The central limit theorem states that the distribution tends toward a Gaussian when there are a large number of variables. In our simplified model, there are only three in the equation for the Sedov radius, so it is somewhat surprising that the distribution of sizes is indistinguishable from log-normal with a modest number

of SNRs ( $\sim 600$ ). For catalogs with a large number of SNRs, one will be able to distinguish between a normal distribution and a non-normal distribution. If the distribution is *not* normal, then one will be able to constrain more parameters and physics about the underlying distributions, rather than merely obtaining information on the mean and variance of the underlying variables. To estimate how large the SNR catalogs under a simplified Sedov model will have to be in order to distinguish from a log-normal distribution, we also include a plot of p-values for each simulation in which  $N$  grows steadily larger in Figure 4; as indicated, normality ( $p \geq 0.05$ ) is lost at a sample size over 600.

A possible reason for the loss of consistency with log-normal stems from recalling that the CLT holds only for as long as the variables remain independently distributed. Clearly, our few variables for the Sedov radius do not meet the criteria as “sufficiently large” and, as shown in eq. 1 and 4, the minimum and maximum lifetimes actually *depend* upon mass and blast energy. Thus, while log-normality is clearly present for samples containing a few hundred SNRs, the fact that the Sedov radius ultimately fails the requirements for the CLT to hold suggests that there should be no reason for this to universally hold for all sample sizes.

Current SNR catalogs are well below  $\approx 600$ , so it is reasonable to assume that the distribution is log-normal. Furthermore, since the size distribution is consistent with being log-normal we can only know about the mean and variance for the distributions of  $E$ ,  $t$ , and  $\rho$ . Therefore, via Bayesian statistical inference, we aim to infer the mean and variance in the log of the ISM density. Recall that Bayes’ theorem states:

$$P(M|D) = \frac{P(D|M)P(M)}{P(D)} \quad (14)$$

where  $P(M|D)$  is our *posterior*,  $P(D|M)$  our *likelihood*,  $P(M)$  our *prior*, and a normalization constant  $P(D)$ . For our purposes, we assume a flat prior such that  $P(M|D) \propto P(D|M)$ . In this context,  $M$  refers to the model parameters and  $D$  the data, such that we seek to calculate the probability of  $M$ , given  $D$ . Considering the log-normality of the Sedov radius, our likelihood function is thus assumed to be the log of a normal distribution function with model parameter  $\log R$ :

$$\log P = -\frac{1}{2} \log \left( 2\pi\sigma_{\log R}^2 \right) - \left( \frac{(\log R - \mu_{\log R})^2}{2\sigma_{\log R}^2} \right) \quad (15)$$

whose parameters depend on the diameter data obtained from the M31 and M33 samples. From this likelihood, we can perform an analysis of the ISM density by modeling  $\rho$  as random, normal distributions. We constrain the statistics of our modeled distributions by calculating the mean and variance of actual explosion data from observed and physical properties of CCSN as found in [Hamuy \(2003\)](#). SNR lifetimes are calculated via eq. 2, 13, and 1 and we perform our Bayesian scheme on the density for both low ( $7-9M_\odot$ ) and high ( $10-120M_\odot$ ) mass ranges. The results are shown in figures 5 and 6, in which we obtain very narrow variances for  $\log \rho$  for both mass ranges; the mean and variance for combined low and high masses come to  $\mu = -1.33$  and  $\sigma^2 = 0.49$ . Our mean values for the density are consistent with those found in previous models of the WIM, such as [Hill et al. \(2008\)](#) who concluded that WIM gas follows a log-normal density distribution with  $\mu_{\log \rho} \approx -1.52$ . [Berkhuijsen & Fletcher \(2008\)](#) also provide supporting evidence that densities in the diffuse ISM are log-normally-distributed, using dispersion and emission measure data derived from pulsar samples. The authors conclude that this behavior is typical for random, non-linear processes such as turbulence.

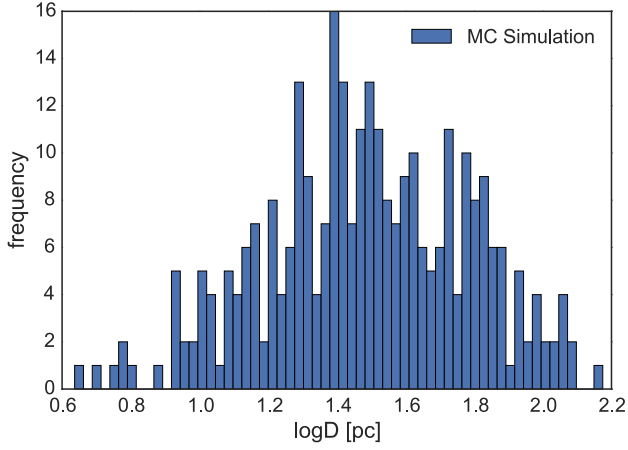


**Figure 2.** Monte Carlo scheme for Sedov radius (in the log), for  $N=300$ . Log-normality is therefore well-produced in the theoretical framework of the simple Sedov radius. P-value  $\approx 0.23$ .

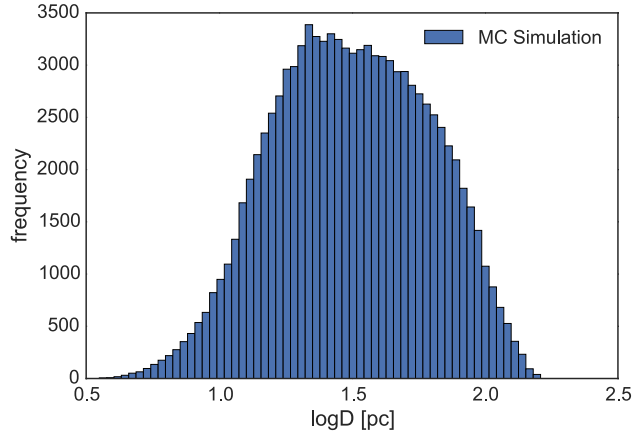


**Figure 3.** Monte Carlo scheme for Sedov radius (in the log), for  $N=100000$ . Note the loss of log-normality when sample grows arbitrarily large, thereby granting additional information on the statistics, such as kurtosis or skewness (clearly present).

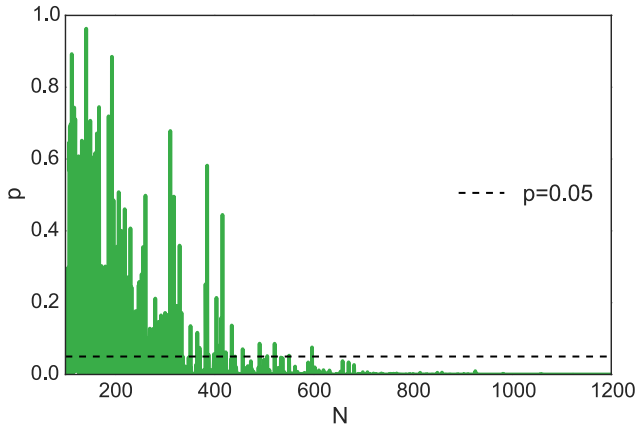


**Figure 4.** P-values versus  $N$ . Distribution becomes inconsistent with log-normal for sample sizes larger than 600.

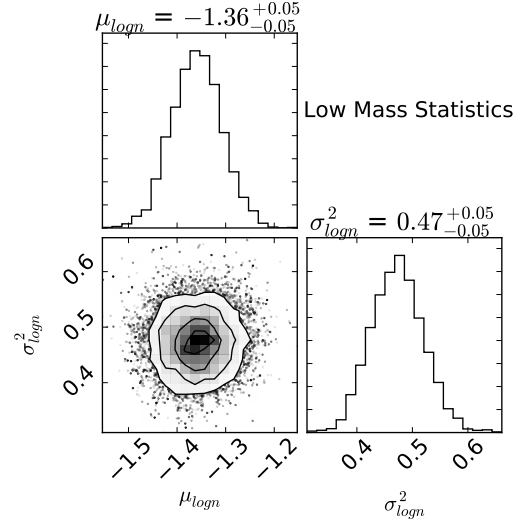


**Figure 5.** Mean particle density  $\mu_{\log n} = -1.36$  and variance  $\sigma_{\log n}^2 = 0.47$ . The small variance in these simulated distributions appears to be consistent with the analysis of the SNR data.

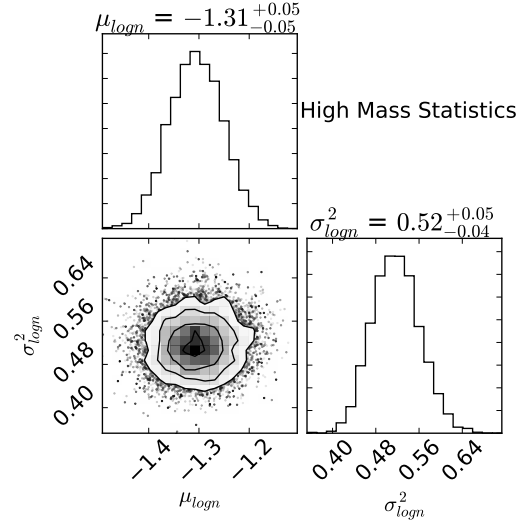


**Figure 6.** Mean particle density  $\mu_{\log n} = -1.31$  and variance  $\sigma_{\log n}^2 = 0.52$ . Variance is evidently insensitive to SNR progenitor mass.

Our modeling suggests that the range of densities is narrow; while this may seem peculiar, there may be underlying, theoretical explanations that we consider in the next section. Additionally, our narrow density distribution is empirically consistent with recent efforts by [Gatto et al. \(2016\)](#), who studied interactions between supernovae and the multi-phase ISM via FLASH hydrodynamic simulations. As part of this study, the authors calculated density statistics for two runs related to SN rates in different density environments. They reported a mean density  $\bar{n}_{SN} \approx 0.07 \text{ cm}^{-3}$  with standard deviation  $\sigma_{SN} = 0.9$  for one run, and  $\bar{n}_{SN} \approx 0.09 \text{ cm}^{-3}$  with  $\sigma_{SN} = 1.1$  for the other; their simulated results suggest that SNRs generally encounter low-density surrounding environments. This is also supported by [Kim & Ostriker \(2016\)](#) who report that high-resolution models (via TIGRESS) produce large fractions of cluster SNe in low-density regions ( $n < 0.1 \text{ cm}^{-3}$ ).

Comparisons with [Sarbadhicary et al. \(2017\)](#) yield mixed re-

sults. Though they do not report the inferred ISM density directly, they do report parameters of their model that go into modeling the density. In their attempt to better understand delay time distributions associated with SNRs, Sarbadhicary et al. (2017) sought to model visibility times, thereby requiring an inference of environmental densities. However, rather than simply including the local density as a parameter, they model the density with a smooth disk-like distribution exponential:

$$n_0(z) = \frac{N_H}{\sqrt{\pi}z_0^2} \exp\left(-\frac{z^2}{z_0^2}\right) \quad (16)$$

where  $n_0$  is the volumetric density,  $N_H$  the HI column density,  $z$  the vertical height at which an SNR explodes in a given spatial location (in M33 for their purposes), and  $z_0$  the scale height for a given galactic disk (again M33). Therefore, two parameters exist, which they effectively reduce to one by including the HI column density observations in their analysis.

As the authors did not report a distribution of densities, we must estimate the mean and variance in  $n_0$ , given their mean and variance in  $z_0$ . However, we first note that their ISM density model might be too restrictive. Equation (16) is a very smooth density distribution and does not account for the multiple phases of the ISM. On top of the smooth exponential profile, the real ISM is percolated with large regions of under dense hot gas and small-volume, but high-mass regions of cold, dense gas. There is no way for their model to capture this inherent variation in the densities of the ISM. Furthermore, using the HI column density is problematic for two reasons. One, the HI column density represents one specific phase and temperature of the ISM, and two, the HI column density is an integral quantity. For these two reasons, the distribution in HI column densities is quite narrow and does not represent the inherent variation in ISM densities (Diamond et al. 1989).

We then use their distributions for  $N_H$  and  $z_0$  to estimate  $\sigma_{\log n}^2$  or  $\sigma_{n_0}^2/n_0^2$ . Assume that  $z$  does not vary significantly, with its mean being nearly zero (an assumption based upon the fact that  $z$  is drawn from an exponential distribution). Invoking the definition of variance as a sum of derivatives normalized by  $n_0^2$  yields:

$$\frac{\sigma_{n_0}^2}{n_0^2} = \frac{\sigma_{N_H}^2}{N_H^2} + 4\frac{z^2\sigma_z^2}{z_0^4} + \left(\frac{4z^4}{z_0^4} + \frac{4z^2}{z_0^2} + 1\right)\frac{\sigma_{z_0}^2}{z_0^2} \quad (17)$$

Estimates of these variables can be obtained in a couple ways. We first estimate the values of  $\sigma_{N_H}$ ,  $\mu_{N_H}$ , and  $\sigma_{z_0}$  from a parameter space figure within Sarbadhicary et al. (2017) in which  $\sigma_{N_H} \approx 1.0 \times 10^{21} \text{ cm}^{-2}$ ,  $\mu_{N_H} = 2.5 \times 10^{21} \text{ cm}^{-2}$ , and  $\sigma_{z_0} \approx 100 \text{ pc}$ . We use  $z_0 = 200 \text{ pc}$ , a value stated by the authors in a figure of visibility times versus column density. If we further assume  $\mu_{N_H} \approx N_H$ ,  $\mu_z \approx z$  (in which  $z = 0$ ), and  $\sigma_z^2 \approx z^2$  (by virtue of it being drawn from an exponential distribution), one obtains a normalized variance of  $\sigma_{n_0}^2/n_0^2 \approx 0.41$ , translating to  $\approx 0.077$  for the variance in  $\log n_0$ . This fractional variance is similar to the fractional variance for  $N_H$ , suggesting that the shape of the volume density distribution is determined by the prior of the authors' column density distribution.

Though Sarbadhicary et al. (2017) did not report values for the variance of  $\log n_0$ , private communication revealed an inferred variance of 0.09, similar to the inference reported in this manuscript (S. K. Sarbadhicary and C. Badenes, personal communication, 2017). The mean densities on the other hand are somewhat different. Figures 5 & 6 show that our mean inferred density distribution is  $\mu_{\log_{10}(n)} \approx -1.3$ . For Sarbadhicary et al. (2017),  $\mu_{\log_{10}(n)} \approx 0.5$ , nearly two magnitudes larger. The standard deviation for our distribution is  $\sigma_{\log_{10}(n)} \approx 0.7$ , such that the means are two sigmas

apart in  $\log_{10}(n)$ . The standard deviation in our mean is 0.05, so the differences in the means are quite significant.

However, the fundamental differences between our analysis and that of Sarbadhicary et al. (2017) imply that it is not entirely appropriate to strictly compare results. In particular, we infer the densities from the size distributions and use a very crude model for the lifetime of observability. On the other hand, Sarbadhicary et al. (2017) use a radio light curve model to infer the densities and ignore the sizes. Furthermore, our analysis makes no assumptions about a specific density model. Rather, we simply infer density statistics using the variance obtained from SNR sizes. Alternatively, the density model assumed by Sarbadhicary et al. (2017) is that of a homogenous disk; as the authors note, disk galaxies in general are complicated and inhomogeneous with respect to the ISM, and their model is likely too restrictive. It would be useful, in future work, to observe how density statistics change with the assumption of more realistic and complicated models and how such statistics compare with those obtained by the more elementary avenue in our work.

#### 4 DISCUSSION

These interesting values suggest a narrow derived density distribution that might lead one to consider the possibility that either surveys of supernova remnants are biased towards the warm, ionized medium or that the evolution of SNRs is not dominated by the simple Sedov radius model. However, an example of a non-Sedov model may include the stellar cavities formed before the progenitor explosion via stellar wind. For some time, it has been known that wind-driven mass-loss plays a significant role in the evolution of stars, particularly for massive stars whose end fates result in core-collapse supernovae (Chiosi & Maeder 1986; Maeder & Meynet 2000; Woosley et al. 2002; Smith 2014). Strong radiation pressure launches powerful winds that push the interstellar medium out several parsecs away from the star, forming a pre-explosion cavity between the progenitor and a shell of ISM material. Upon explosion, a minimum ejecta mass of  $6.6M_\odot$  easily overwhelms any surrounding mass left in the stellar cavity; we verify this by considering a relatively low mass-loss rate of  $10^{-6}M_\odot$  (Smith 2014), combined with a wind velocity of 10 km/s, and a lower bound cavity size of 2 pc (to be calculated later). This results in a lower-bound for the mass in the surrounding medium:

$$M_{\text{wind}} = \frac{\dot{M}R}{v} \approx 0.2M_\odot \quad (18)$$

Similarly, an upper bound for high-mass stars can be approximated with a mass-loss rate of  $10^{-4}M_\odot/\text{yr}$ , a wind velocity of 300 km/s, and a cavity size of 20 pc, obtaining  $M_{\text{wind}} \approx 6.5M_\odot$ . Therefore, we obtain a range of surrounding wind masses  $0.2 \leq M_{\text{wind}} \leq 6.5$ , compared to ejecta masses of  $6.6 \leq M_{\text{ej}} \leq 118.6$  such that,  $M_{\text{ej}} > M_{\text{wind}}$ .

With very little medium in the way, the blast wave quickly traverses the cavity in a free expansion phase, and it does not slow down appreciably until it reaches the swept up shell. Once the blast wave reaches the shell, there's enough material in the shell and the circumstellar medium to quickly slow down the evolution from a free expansion to a Sedov-like expansion. Because the blast wave would spend very little time in the free expansion phase inside the wind-swept cavity (see eq. 4), one would detect very few SNRs with sizes less than the wind-swept cavity size. Therefore, the size of the wind-swept cavity presents a minimum size for the SNRs.

A consequence for the size distributions of SNRs in Sedov

expansion immediately follows: a minimum cut-off exists for SNR distributions whose size is determined by the strength of the pre-explosion stellar winds. An estimate of this cut-off can be found through a simple order-of-magnitude calculation. Through ram pressure, the wind blows a bubble in the ISM. Since the ram pressure declines with radius, but the ISM thermal pressure does not, at some point the wind ram pressure drops until it is roughly equal with the ISM thermal pressure. This rough balance in pressures essentially sets the size of the wind-swept cavity. Recall that, for a fluid, the ram pressure is  $P \sim \rho v^2$  where in this case,  $P$  is the pressure of the ISM and  $v$  the velocity of the stellar wind. With the stellar mass-loss rate  $\dot{M} = 4\pi\rho v R^2$ , we can then substitute for the density and derive an estimate for the radius of the stellar cavity:

$$R \sim \sqrt{\frac{\dot{M}v}{4\pi\rho}} \quad (19)$$

Thus, for mass-loss rates of  $10^{-6}M_{\odot}/\text{yr}$  to  $10^{-4}M_{\odot}/\text{yr}$  (Smith 2014), an ISM pressure of  $P = 3000k_B \text{ K/cm}^3$ , and a relatively-slow wind velocity of  $v = 30 \text{ km/s}$ , one obtains a range of cavity sizes from  $\approx 2$  to  $20 \text{ pc}$ . This is remarkably similar to the lower end of the SNR size distribution in Figure 1. Yet, we have already shown that the distribution of densities is also consistent with the WIM. Either SNRs are biased to a narrow range of radii (because they trace the WIM) or they all have windblown cavities of order 2 to  $20 \text{ pc}$ .

Additionally, one might hope to use SN rates for M31 or M33 to assess whether SNR catalogs are biased. However, we find that the current estimates for SN rates are far too uncertain to provide such a constraint. The most recent efforts characterize SN rates as a function of specific star formation rate (sSFR) (Graur et al. 2015; Botticella et al. 2016). With this correlation we can estimate SN rate for M31 and with a SNR lifetime we can estimate the number of SNRs.

The sSFR for M31 from recent estimates is  $6.8 \times 10^{-12} M_{\odot}^{-1}\text{yr}^{-1}$  plus or minus about 20%, which we calculate using M31's recent star formation history (Lewis et al. 2015) and stellar mass (Sick et al. 2015) from the M31 Panchromatic Survey. The correlation between type-II SN rate and sSFR is  $\log(R_{\text{II}}) = \log(A_s)B_s \log(\text{sSFR})$ , where  $A_s = 7.9^{+4}_{-3.4}$  and  $B_s = 1.33^{+0.41}_{-0.35}$  (Graur et al. 2015). The fraction of CCSNe that are II is  $0.693 \pm 0.067$  (Li et al. 2011; Shivvers 2016).

Given these estimates, the most likely SN rate for M31 is  $0.0016 \text{ SNe/yr}$  with an uncertainty in the range between  $0.0005$  and  $0.0058 \text{ SNe/yr}$ . To calculate the number of expected SNRs, we need to know the typical lifetime of a SNR. A good guess would put this somewhere between  $10^4$  and  $10^5$  years. The geometric mean for this best guess is  $3 \times 10^4$  years. Therefore, the best prediction for the number of SNRs in M31 is 50. However, our best estimates for the uncertainty allows a range between 10 and 250 SNRs. Clearly, predictions for the number of expected SNRs is far too uncertain to constrain whether current SNR catalogs are biased and missing SNRs. In fact, historical trends suggest that every new attempt to find SNRs yields yet more SNRs (Plucinsky et al. 2008; Long et al. 2010; Lee & Lee 2014).

## 5 CONCLUDING REMARKS

We use the size distributions of SNRs to infer the properties of the ISM. If we consider the simplest and most straightforward model, the Sedov phase, then the narrow size distribution implies a narrow

range of densities. Either SNR surveys are biased towards the warm, ionized medium, or the most obvious and simple model for SNR evolution is incorrect.

Though our statistical analysis is straightforward and simple, this conclusion seems robust and may provide insight into SNR evolution and observational biases. Quite simply, the distribution of SNR sizes is log normal and narrow. The log-normal character is consistent with the most common assumption made about SNR evolution; the Sedov phase dominates the visible phase of SNR evolution. Even though there are only three random variables in the Sedov radius, simple Monte Carlo simulations demonstrate that one can reproduce these log-normal distributions for appropriately-sized SNR samples, less than  $\sim 600$  SNRs. The puzzling result of these studies is that, assuming a simple Sedov mode for the SNR blast wave, both data and simulations reveal an unusually-small variance for the surrounding ISM density.

Our primary motivation in inferring the density distribution is to assess whether there is a bias in SNR catalogs. Given our result, we are now in a position to address whether there is a bias in SNR catalogs. First of all, it is not clear whether the density distribution is actually narrow or if there are other mitigating factors; for example, SNR evolution may not be dominated by the Sedov phase. However, the independent results of two groups support our conclusion that the density distribution is narrow. Gatto et al. (2016) simulated SNe in galactic simulations and found that most SNe explode in the same range of densities that we infer from observations. In addition, Sarbadhicary et al. (2017) used radio emission to infer the radio emission lifetime and ambient densities (omitting inference from SNR sizes, in contrast to our method). Both authors, in some fashion, estimated the number of SNRs below detection limits and ambient densities, with Gatto et al. (2016) obtaining results similar to our own and Sarbadhicary et al. (2017) obtaining mean densities nearly two orders of magnitude higher. We find that these results are a direct and simple consequence of the narrow diameter distribution in the context of Sedov evolution and, taken together, suggest that SNe tend to explode in the WIM. In this interpretation, either *all* SNe explode in the WIM, or we are only seeing the ones that do.

Sarbadhicary et al. (2017) analyzed a single M33 radio survey of SNRs, and they found that 30-40% of actual SNRs fall below the detection limits of current radio surveys. Taken at face value, their results suggest that current catalogs contain most of the SNRs in a galaxy. This implies that most SNe explode in the WIM, and we are not missing the dominant fraction of SNRs.

Even if current catalogs contain most of the SNRs, the missing SNRs could represent a bias against finding certain SNRs. For example, if the most massive stars exploded in HII regions, then these might escape detection. Due to the scarcity of very massive stars, this reduction could represent a small fraction in the total number of SNRs. For example, if all progenitors above  $35M_{\odot}$  exploded in HII regions, then this would result in only an approximate 14% reduction in the total number of SNRs from our chosen catalogs. Given our rough estimates, it is unlikely that we can determine whether  $\sim 10\%$  of SNRs are missing. Therefore, there is a possibility that SNRs associated with the most massive progenitors are missing from catalogs.

In an attempt to constrain a mass dependence scenario, we applied our inference technique as a function of progenitor mass. Jennings et al. (2014) published progenitor masses for the SNRs that we consider; in figures 5 and 6, we infer the density distributions for the high mass and low mass progenitors. We do not find a statistical difference between low mass and high mass progenitors, thus suggesting that if there is a bias it is largely independent of

mass, or the mass dependence bias does not dominate the SNR statistics.

Another possibility is that the evolution of SNRs in the Sedov phase does not entirely determine the shape of the SNR size distribution. Cavities blown by the progenitor’s stellar winds may partially account for the small variance in that they may provide a minimum size for SNRs.

In summary, we find that a simple statistical inference of the SNR size distribution provides an interesting constraint on the evolution of SNRs. Either SNe mostly explode in the WIM, there is a bias to only *observing* SNRs that explode in the WIM, or the most obvious assumption about SNR evolution—that their visibility is dominated by the Sedov phase—is incorrect. Although our simple analysis does not definitively distinguish between these options, it does highlight potential problems with using SNR catalogs to understand SN physics. None the less, SNRs remain important markers of recent SNe, and so SNR catalogs continue to be some of the most important catalogs for understanding SN physics.

To harness the full potential of SNR catalogs, we suggest the following avenues of investigation. First of all, we simply require more data; identifying more SNRs will help to further constrain the distribution of SNR sizes. If we can obtain thousands of SNRs, then one will be able to model the distribution beyond log-normal, allowing us to infer more parameters than the mean and variance. This will in turn provide more constraints on theoretical models for SNR evolution. Furthermore, these catalogs should be defined using the most robust SNR identification techniques. Second, we require more data about the environments of SNRs that are independent of SNR evolutionary models. Finally, we need better SNR evolutionary models and the best way to achieve this would be to better understand the evolution of individual SNRs. This will require a concerted effort between detailed observations of local SNRs and detailed evolutionary modeling. Together, more data and better theoretical modeling will enable us to constrain potential biases in SNR catalogs, allowing us to better use them to infer the physics of SNe.

## ACKNOWLEDGMENTS

We thank Carles Badenes for suggesting that we investigate the size distributions of supernova remnants. This material is based upon work supported by the National Science Foundation under Grant No. 1313036.

## REFERENCES

Asvarov, A. I. 2014, *A&A*, 561, A70  
 Badenes, C. & Maoz, D. & Draine, B. T. 2010, *MNRAS*, 407, 1301  
 Bandiera, R., & Petruk, O. 2010, *A&A*, 509, A34  
 Berkhuysen, E.M. 1986, *A&A*, 166, 257B  
 Berkhuysen, E.M. 1987, *A&A*, 181, 398B  
 Berkhuysen, E.M. & Fletcher, A. 2008, *MNRAS*, 390, L19  
 Blondin, J. M., & Wright, E. B. & Borkowski, K. J. & Reynolds, S. P. 1998, *ApJ*, 500, 342  
 Botticella, M. T. et al. 2016, preprint, (arXiv:1610.01176)  
 Braun, R. & Walterbos, R. A. M. 1993, *A&AS*, 98, 237  
 Cappellaro, E. & Evans, R. & Turatto, M. 1999, *A&A*, 351, 459  
 Cioffi, D. F. & McKee, C. F. & Bertschinger, E. 1988, *ApJ*, 334, 252  
 Chiosi, C. & Maeder, A. 1986, *A&A*, 152, 329C  
 Dalcanton, J.J. & Williams, B. F. & Lang, D. et al. 2012, *ApJS*, 200, 18  
 Diamond, P. J. et al. 1989, *ApJ*, 347, 302  
 Foreman-Mackey, D. & Hogg, D. W. & Lang, D. & Goodman, J. 2013, *PASP*, 125, 306

Fusco-Femiano, R. & Preite-Martinez, A. 1984, *ApJ*, 281, 593F  
 Gatto, A. et al. 2016, preprint, (arXiv:1606.05346)  
 Graur, O. & Bianco, F. B. & Modjaz, M. 2015 *MNRAS*, 450, 905G  
 Faucher-Giguère C.-A. & Kaspi, V. M. 2006 *ApJ*, 643, 332  
 Gogarten, S. M. et al. 2009, *ApJ*, 703, 300  
 Gordon, S. M. et al. 1998, *ApJS*, 117, 89  
 Hamuy, M. 2003, *ApJ*, 582, 905  
 Hill, A. S. et al. 2008, *ApJ*, 686, 363  
 Hughes, J. P. & Helfand, D. J. & Kahn, S. M. 1984, *ApJ*, 281L, 25H  
 Jennings, Z. G. et al. 2014, *ApJ*, 795, 170  
 Jennings, Z. G. et al. 2012, *ApJ*, 761, 26  
 Kim, C.-G. & Ostriker, E. C. 2016, preprint, (arXiv:1612.03918)  
 Lee, J. H. & Lee, M. G. 2014, *ApJ*, 793, 134L  
 Lee, J. H. & Lee, M. G. 2014, *ApJ*, 786, 130  
 Lewis, A. R. et al. 2015, *ApJ*, 805, 183L  
 Li, W. et al. 2011, *MNRAS*, 412, 1441L  
 Long, K. S. et al. 2010, *ApJS*, 187, 495  
 Maeder, A. & Meynet, G. 2000, *ARA&A*, 38, 143M  
 Magnier, E. A. & Prins, S. & van Paradijs, J., et al. 1995, *A&AS*, 114, 215  
 Magnier, E. A. et al. 1997, *ApJ*, 490, 649  
 Maoz, D. & Badenes, C. 2010, *MNRAS*, 407, 1314  
 Massey, P. et al. 2006, *AJ*, 131, 2478  
 Mathewson, D.S. & Ford, V. L. & Dopita, M. A. & Tuohy, I. R. & Long, K. S. & Helfand, David J. 1983 *ApJS*, 51, 345M  
 Murphy, J. W. et al. 2011, *ApJ*, 742, L4  
 Plucinsky, P. P. et al. 2008, *ApJS*, 174, 366  
 Rahmani, S. & Lianou, S. & Barmby, P. 2016 *MNRAS*, 456, 4128R  
 Sarbadhicary, S. K. & Badenes, C. & Chomiuk, L. & Caprioli, D. & Huizenga, D. 2016, *MNRAS*, 464, 2326  
 Sick, J. et al. 2015, *IAU Symposium*, 311, 82S  
 Smith, N. 2014, *ARA&A*, 52, 487S  
 Shivvers, I. et al. 2016, preprint, (arXiv:1609.02922)  
 Truelove, J. K. & McKee, C. F., 1998, *ApJS*, 120, 299  
 Verley, S. & Corbelli, E. & Giovanardi, C. & Hunt, L. K. 2009, *A&A*, 493, 453  
 Williams, B. F. et al. 2014 *ApJ*, 791, 105  
 Woosley, S. E. & Heger, A. & Weaver, T. A. 2002, *Rev. Mod. Phys.*, 74, 1015